JOURNAL OF PROPULSION AND POWER
Vol. 25, No. 1, January–February 2009

Thrust Performance of a Microwave Rocket Under Repetitive-Pulse Operation

Yasuhisa Oda,* Teppei Shibata,† and Kimiya Komurasaki‡
University of Tokyo, Chiba 277-8561, Japan
and
Koji Takahashi,§ Atsushi Kasugai,§ and Keishi Sakamoto¶
Japan Atomic Energy Agency, Ibaraki 311-0193, Japan

DOI: 10.2514/1.37623

An experiment was conducted on a microwave rocket (repetitive-pulse millimeter-wave-beam-powered thruster) with repetitive pulses. A thruster model with a forced-breathing system was used. The forced-breathing system supplies fresh air from the thrust wall into the thruster. The pressure histories in the thruster were measured and the propagation velocity of the shock wave and the thrust impulse were deduced. Results show that although the propagation velocity was identical to the result for the single-pulse operation at the first pulse, the propagation velocity increased after the second pulse. Similarly, the impulse decreased after the second pulse. The dependence of the propagation velocity of the shock wave and the thrust performance on the partial-filling rate of the fresh air was compared with that of the thrust-generation model with a forced-breathing system. The experimental results showed good agreement with those obtained using the model.

Nomenclature

A	=	area of the thruster
C_m	=	momentum coupling coefficient
c_p	=	isobaric specific heat
f	=	pulse repetition frequency
I	=	thrust impulse
I_{osc}	=	thrust-generated by pressure oscillation
I_{single}	=	thrust impulse at single-pulse operation
L	=	total length of the thruster
M_1	=	Mach number of the shock wave
M_{3c}	=	Mach number of the rarefaction wave relative to the thrust wall
p_0, T_0	=	gas pressure and temperature at the ambient
p_1, T_1	=	gas pressure and temperature at the initial state in the thruster
p_2, T_2	=	gas pressure and temperature behind the shock wave
p_3, T_3	=	gas pressure and temperature behind the heating region
p_4, T_4	=	gas pressure and temperature at the thrust wall
S	=	microwave power density
t_{plateau}	=	time duration that high pressure at the thrust wall is kept
U	=	propagation velocity of shock wave
u	=	flow velocity in the forced-breathed thruster
u_2	=	local flow velocity behind the shock wave relative to the heating region
V_{fresh}	=	volume of supplied fresh air in the thruster
γ	=	specific heat ratio
η	=	efficiency of microwave absorption by plasma
ρ_2	=	gas density behind the shock wave
τ	=	microwave-pulse duration

Received 19 March 2008; revision received 25 June 2008; accepted for publication 14 July 2008.

*Ph.D. Student, Department of Advanced Energy, 5-1-5 Kashiwa-no-ha, Kashiwa. Student Member AIAA.

†Graduate Student, Department of Advanced Energy, 5-1-5 Kashiwa-no-ha, Kashiwa.

‡Associate Professor, Department of Advanced Energy, 5-1-5 Kashiwa-no-ha, Kashiwa. Member AIAA.

§Assistant Principal Researcher, Fusion Research and Development Directorate, 801-1 Mukoyama, Naka.

¶Senior Principal Researcher, Fusion Research and Development Directorate, 801-1 Mukoyama, Naka.

I. Introduction

BEAMED-ENERGY propulsion (BEP) is a propulsion system that obtains propulsive energy using an electromagnetic wave beam. Because propulsive energy is provided by beamed energy that is transmitted from outside, the vehicle needs to carry no energy source and thereby achieves a high payload ratio. Although the concept of BEP was proposed early, few scientific works were done before the 1960s because of the lack of appropriate energy sources. However, because of the invention of high-power beam sources such as lasers, experimental research on BEP was begun [1]. Studies of BEP are now being conducted by many groups using lasers [2–4]. For BEP, once the energy beam station is built, it is useful for many launches. The beam oscillator development cost is predominant when there are few launches. The development cost for microwave oscillators is expected to be 2 orders of magnitude lower than that of a laser, because a gigawatt-class oscillator is achievable by clustering existing high-power oscillators using phased-array technology. Consequently, microwave BEP is anticipated to achieve lower launch costs with fewer launch counts than with laser BEP [5].

Studies of microwave BEP also began a few decades ago. In the 1980s, Knecht and Micci [6] conducted an analysis of microwave rocket systems. In the thruster, the propellant is heated by microwaves in the dielectric chamber; it is exhausted by a nozzle, similarly to a chemical rocket. Its specific impulse was estimated to 2000 s using hydrogen propellant. Batanov et al. [7] also conducted analyses of a microwave rocket using $\lambda = 10$ mm microwaves. The rocket nozzle was made from dielectric material to provide microwave power in the rocket. Its thrust performance was estimated as 50 W/kg. Parkin and Culick [8] proposed the microwave thermal rocket. In their concept, high-power microwaves heat a propellant in the dielectric heat exchanger tube; the heated propellant is exhausted through a nozzle, similarly to a conventional rocket. Bruccoleri et al. [9] measured the temperature of helium in a mullite tube using 2.45 GHz microwaves. These early studies are based on steady operation. Indeed, laser propulsion using atmospheric discharge by repetitive pulses was proposed and examined. It obtained high thrust performance under atmospheric conditions because laser-supported

detonation under a high-power laser beam achieves high-efficiency energy conversion.

A repetitive-pulsed microwave-beaming propulsion system using microwave breakdown is proposed in this study. Pulsed plasma produced using a high-power microwave pulse drives a blast wave. A thruster exhausts the blast wave and acquires impulsive thrust force. This system is called a microwave rocket. The concept of the microwave rocket has an advantage in its simple design. A thruster merely comprises a focusing reflector substituted for an exhaust nozzle. In addition, a microwave rocket can achieve a high payload ratio, because the microwave rocket uses atmospheric air as a propellant during flight in the atmosphere. Nakagawa et al. [10] conducted a single-pulse experiment using a conceptual thruster of a microwave rocket with a 1 MW microwave beam. The measured momentum coupling coefficient C_m, defined as a ratio of propulsive impulse to input power, was greater than 400 N/MW. The atmospheric millimeter-wave plasma drives a shock wave when its ionization front propagates supersonically [11].

Thrust performance under multipulse operation was measured with both a vertical flight experiment and a horizontal fixed experiment using pressure gauges. For 10–60 Hz pulse repetition with two pulses, the impulse imparted at each pulse and its C_m were deduced using the thruster model with a tube. Consequently, at the second pulse, C_m decreased for all repetition conditions. Reference [12] presents the conclusion that the decrease in C_m was caused by hot air remaining in the thruster [12]. When the microwave rocket flies at the ramjet flight mode, fresh air is supplied from the front side of the engine, thereby enhancing its air-refilling process. Therefore, the performance degradation needs to be avoided or minimized. To simulate airbreathing conditions during the flight for this study, the microwave-beaming thruster with a forced-breathing system (which provides fresh air from the thrust wall) was designed to resemble ramjet mode. The thrust-generation model with a forced-breathing system was developed. The pressure history in the thruster was measured and the propagation velocity of the shock wave and the impulsive thrust were deduced for each pulse under repetitive-pulse operation. The thrust performance under multipulse operation was estimated and compared with the thrust-generation model with the forced-breathing system.

II. Thrust-Generation Model

The thrust-generation model of a microwave rocket is explained using an analogy to a pulse detonation engine (PDE). In a PDE, a detonation wave starts from a thrust wall and propagates to the exit [13,14]. In a microwave rocket, a shock wave supported by the microwave plasma propagates in the tube instead of a detonation wave.

The energy conversion process in a microwave rocket resembles the shock wave driven by a deflagration wave in the closed-end tube. In the model, the shock wave is even driven by the microwave plasma when the ionization front of plasma is detached from the shock wave with subsonic propagation of the front. This is because the ionization front of plasma absorbs microwave power and its heating produces a heated compression wave, which propagates to the tube exit. Because the local sonic velocity of heated air is greater than that of the initial tube air, it is mutually combined and finally becomes a normal shock wave. As a result, the shock wave propagates in the tube, even detaching from the heating region. Because microwave power is absorbed at the ionization front that propagates in the subsonic velocity, isobaric heating is caused, similar to a deflagration wave. Behind the isobaric heating region, the decelerating rarefaction wave follows because of the closed-end tube. A constant-pressure region is formed between the end and the tail of the rarefaction wave. The pressure at the thrust wall is kept constant until the reflected expansion wave arrives at the thrust wall. Air in the thruster is scavenged with pressure oscillation after pressurized air was exhausted. A schematic of the distribution of regions is presented in Fig. 1. At the region behind the normal shock, pressure and temperature are represented, respectively, as p_2 and T_2. Similarly, at the region heated by plasma, they are p_3 and T_3; at the constant region behind the rarefaction wave, they are p_4 and T_4. Equations of pressure and temperature relations between regions are presented in Table 1.

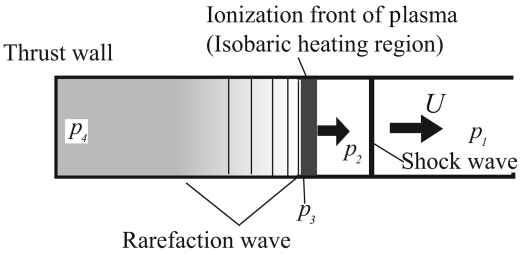

Fig. 1 Propagation of a shock wave in the thruster.

A thrust-producing model based on shock wave propagation was proposed and measurements of the pressure histories in the thruster were described in [15]. Thrust is estimated from the pressure histories in those experiments; results show good agreement with thrust measurements from flight experiments [15].

During the pulse interval, the air in the thruster is partially replaced by the forced-breathing system. The fresh airflow provided from the thrust wall replaces the hot air remaining in the thruster. The fractional rate of the fresh-air-filling in the thruster by forced breathing depends on the parameters, the thruster length L, the pulse repetition frequency f, and the bulk velocity of forced airflow in the thruster u. Therefore, the partial-filling rate of forced breathing is defined as

$$\frac{V_{\text{fresh}}}{LA} = \frac{Au/f}{LA} = \frac{u}{Lf} \tag{1}$$

In the forced-breathing system, the initial temperature in the thruster was controlled by the partial-filling rate. In the thrust-generation model with a forced-breathing system, the initial condition of the cycle was represented by a mixture of fresh air and hot air remaining in the thruster. Therefore, weighted mean properties in the thruster express representative properties of the initial condition. The temperature of the hot air remaining in the thruster was assumed to the temperature of the exhausted air T_4. The initial properties in the thruster for repetitive-pulsed operation was calculated using the partial-filling rate by

$$p_1 = p_0, \qquad T_1 = \frac{u}{Lf}T_0 + \left(1 - \frac{u}{Lf}\right)T_4 \tag{2}$$

The distribution and history of pressure in the thruster were analyzed for a cycle by iterating the calculation using Eq. (2) and the equations listed in Table 1. The analyzed pressure history was applied into the calculation of impulsive thrust.

Total impulsive thrust I for a single-cycle operation is calculated as

Table 1 Equations of shock wave and heating-region relations

	Pressure relations	Temperature relations
Normal shock wave	$\frac{p_2}{p_1} = 1 + \frac{2\gamma}{\gamma+1}(M_1^2 - 1)$	$\frac{T_2}{T_1} = [1 + \frac{2\gamma}{\gamma+1}(M_1^2 - 1)][\frac{2+(\gamma-1)M_1^2}{(\gamma+1)M_1^2}]$
Isobaric heating region	$p_2 = p_3$	$T_3 = T_2 + \frac{\eta S}{c_p u_2 \rho_2}$
Rarefaction wave	$\frac{p_4}{p_1} = \frac{p_3}{p_1}[1 - \frac{\gamma-1}{2}M_{3C}]^{\frac{2\gamma}{\gamma-1}}$	$\frac{T_4}{T_1} = \frac{T_3}{T_1}[1 - \frac{\gamma-1}{2}M_{3C}]^2$

$$I = \int (p - p_0) A \, dt = (p_4 - p_0) A t_{\text{plateau}} - I_{\text{osc}} \tag{3}$$

where A is the area of the thrust wall, t_{plateau} is the duration time of constant pressure at the thrust wall, and I_{osc} is the negative thrust caused by pressure oscillation after exhaust. The negative thrust in the microwave rocket was observed in our previous study and the relation $I_{\text{osc}} \sim 0.25(p_4 - p_0)At_{\text{plateau}}$ was applied [15].

The dependence of the shock wave velocity and thrust performance on the partial-filling rate was estimated using these equations and the measurement result of the Mach number of the shock wave under the single-pulse operation.

III. Experimental Apparatus

A. Microwave Generator

A high-power gyrotron was used as a microwave-beam generator. It was developed by the Japan Atomic Energy Agency as a microwave power source for electron cyclotron heating and the electron cyclotron current drive system of the International Thermonuclear Experimental Reactor. Its frequency is 170 GHz; its nominal output power is up to 1 MW. During single-pulse operation, the microwave-pulse duration is variable from 0.1 ms to continuous-wave operation. Its power remains almost constant during the pulse duration [16,17].

In the gyrotron, microwaves are oscillated through the interaction between the accelerated electron beams and the electromagnetic waves by a cyclotron resonance maser in a cavity with magnetic fields. In this study, to provide microwave pulses repetitively, the acceleration voltage of an electron beam was modulated and the oscillation mode in the cavity was controlled. The interval time duration between pulses was set to 20–50 ms. A typical power history is presented in Fig. 2. The pulse duration τ and peak power P of each pulse were, respectively, about 1.7 or 3.4 ms and 270 kW. Pulse duration τ was selected depending on thruster length L to achieve $U\tau > L$. A microwave beam was transmitted through a corrugated waveguide to the experiment site. The output microwave beam was a fundamental Gaussian beam with a 20 mm waist.

B. Measurement Apparatus for Pressure History

Figure 3 shows the conceptual thruster model composed of a cylindrical tube with a conical nose. The microwave beam was input from the tube exit and focused on the centerline by the conical-nose reflector, initiating plasma. A shock wave and an ionization front propagated through the cylindrical tube, absorbing the microwave beam during the pulse. The total length of the thruster was varied from 190 to 590 mm; the tube diameter was 60 mm. This thruster model has the same thruster shape as that used in the flight experiment described in [11].

Pressure histories in the thruster were measured to deduce the average velocity of a shock wave. Figure 3 shows that two pressure gauges (603B; Kistler) were mounted at the cylindrical tube. One is set near the thrust wall; another is set near the exit. The average

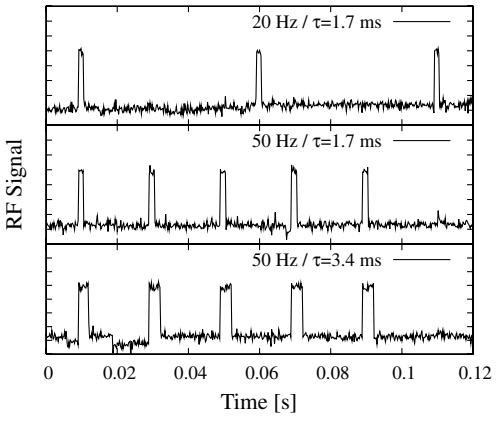

Fig. 2 Typical microwave-pulse records under multipulse operation.

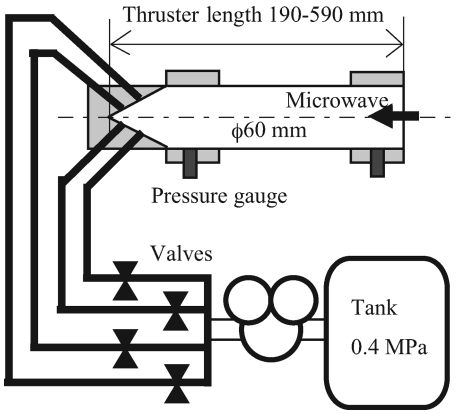

Fig. 3 Thruster model with breathing system and pressure measurement.

velocity of the shock wave in the thruster was calculated from the difference of the arrival time of the shock wave at each gauge.

Fresh air was supplied from the thruster wall. Four flexible tubes were connected to the conical nose and a high-pressure tank. Four electrically controlled valves (AB41-03-4; CKD Corporation) controlled the airflow in each tube. The flow velocity of the fresh air in the thruster was controlled by the number of valves to control. Pressure of the high-pressure tank was kept at 0.4 MPa using a pressure regulator. Each valve controls 0.0074 kg/s of the airflow and the air was supplied from conical-nose wall into the thruster, perpendicularly to the thruster axis. The designed flow speed u was varied from 2.5 to 10 m/s. The flow velocity was estimated from the number of controlled valves and mass flow in the valve. During the multipulse operation, controlled valves were set open to supply continuous fresh airflow. The ambient thrust generated by maximum airflow was estimated at 0.3 N.

The dependence of velocities of the shock wave in the thruster was measured to observe the effect of the forced-breathing system. Because the speed of fresh airflow in the thruster by forced breathing is lower than the shock wave, the velocity had a slight dependence on the airflow speed.

IV. Experimental Result

A. Thrust Impulse Dependence on Each Pulse

The pressure history in the thruster was measured under multipulse operation. Operation of the pulse repetition at 20–50 Hz was carried out for approximately a 0.1 s duration. During the operation, 3–5 pulses were provided to the thruster. Table 2 shows the list of experimental conditions. Figure 4 shows the pressure history obtained at each pulse with a 10 m/s flow and without flow. At each pulse, the shock wave and plateau pressure p_4 were observed in the thruster. After a few pulses were input in the condition without airflow, both p_4 and plateau time duration t_{plateau} were decreased. On the other hand, pressure history with airflow showed a similar history to the first pulse. The propagation velocities of a shock wave observed at each pulse input are presented Fig. 5; the thrust impulses are shown in Fig. 6. The propagation velocity of the shock wave was equal to that of the result of the single-pulse operation when the first pulse was input at $t = 0$ s. In the second pulse and thereafter, the propagation velocity was increased and the propagation velocity was steady for later pulses. Therefore, the operation is expected to be

Table 2 List of experimental conditions

Thruster length L	Airflow speed u	Pulse duration τ	Partial-filling rate u/Lf
190 mm	2.5 m/s	1.7 ms	0.26–0.66
290 mm	0, 2.5 m/s	1.7 ms	0.17–0.43
390 mm	0–10 m/s	3.4 ms	0.16–1.28
490 mm	2.5 m/s	3.4 ms	0.10–0.26
590 mm	0, 10 m/s	3.4 ms	0.2–0.84

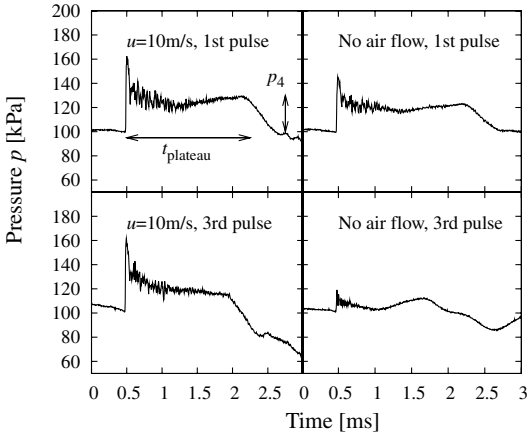

Fig. 4 Pressure history near the thrust wall and its dependence on the pulse number and airflow speed.

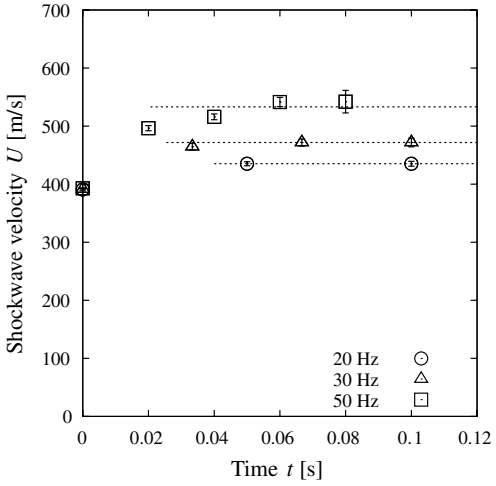

Fig. 5 Dependence of the propagation velocity of the shock wave on the pulse; $L = 290$ mm thruster.

steady after the third pulse. The propagation velocity U at a multipulse operation was defined as the average of the velocities obtained after the third pulse.

Similar to the propagation velocity of the shock wave, the thrust impulse imparted at each pulse has identical dependence. The impulse decreased at the second pulse and the steady impulse was also obtained at later pulses. During steady operation, the

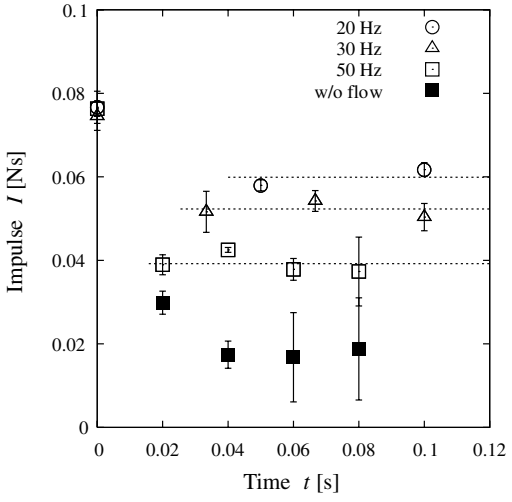

Fig. 6 Dependence of the thrust impulse on each pulse; $L = 290$ mm thruster.

average of the thrust impulses obtained at later pulses was defined as impulse I at the multipulse operation. The result of thrust impulse without airflow at 50 Hz operation is also depicted in Fig. 6. In this condition, the thrust impulse decreased to 15% of the single-pulse result.

Finally, pressure histories under the repetitive-pulse operation for 1 s duration were measured. The repetition frequencies were set as 20 and 50 Hz. Figure 7 shows the velocity of the shock wave formed at each pulse for 20 and 50 Hz repetitions. The velocity of the shock wave was saturated after a few pulses.

Thrust impulses estimated from the pressure history are shown in Fig. 8. The thrust impulse was smaller than the impulse at the first pulse and the thrust impulse became steady at later pulses. Consequently, steady operation was achieved for both frequencies.

B. Dependence of Thrust Performance on the Partial-Filling Rate

The average propagation velocity of the shock wave and the imparted impulse were measured for various conditions to validate the model. The conditions of the airflow velocity were $u = 2.5$ m/s for the thruster length $L = 190$–490 mm and $u = 10$ m/s for the thruster length $L = 390$ mm. Figure 9 shows the dependence of the propagation velocity of the shock wave on the partial-filling rate: the experimental results on the propagation velocity showed good agreement with the predicted dependence by the thrust-generation model based on the normal shock wave driven by atmospheric plasma under a partial-filling condition.

Because the thrust impulse obtained at each cycle depends on the thruster length, the normalized thrust impulse was calculated to compare the dependency of the thrust performance on the partial-filling rate for different thruster lengths. Normalized impulse I/I_{single} was defined as the ratio of the average impulse at multipulse

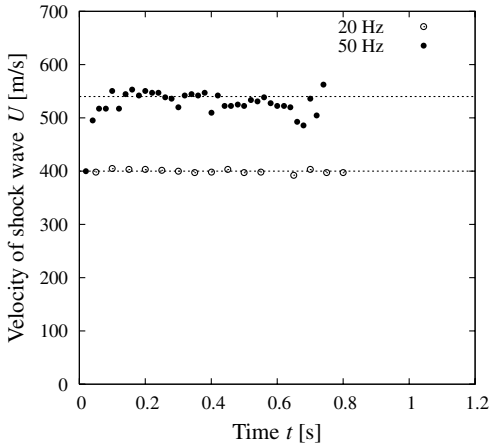

Fig. 7 Estimated velocity of the shock wave at each pulse.

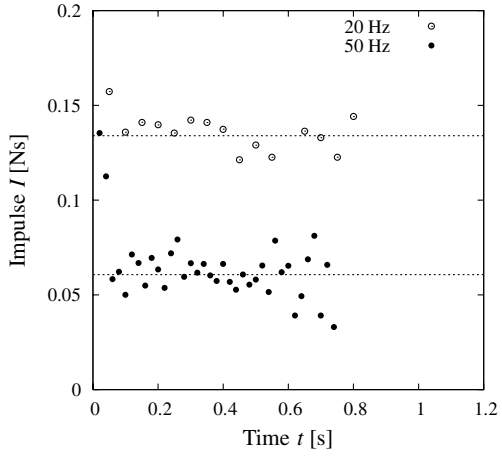

Fig. 8 Estimated thrust impulse at each pulse.

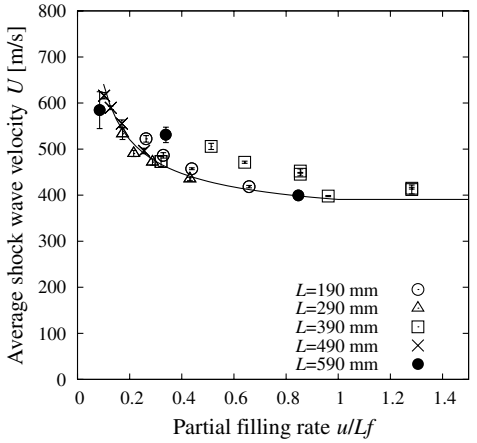

Fig. 9 Dependence of average propagation velocity of the shock wave on the partial-filling rate.

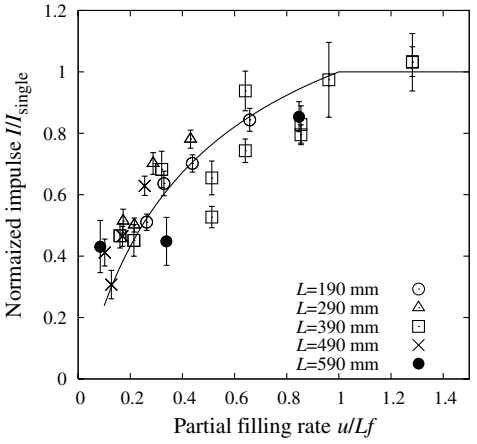

Fig. 10 Dependence of the normalized thrust impulse on the partial-filling rate.

operation to that at the single-pulse operation. Figure 10 shows the dependence of the normalized impulse on the partial-filling rate and the thruster length. In the graph, the partial-filling rate u/Lf was used for the horizontal axis. As presented in Fig. 10, similar to the shock wave, the experimental result on the thrust impulse showed good agreement with the predicted dependence.

Finally, when the partial-filling rate becomes unity, the normalized thrust impulse I/I_{single} becomes unity, verifying that the microwave rocket is operable under a sufficient filling process without decreased performance.

V. Conclusions

In multipulse operation with a forced-breathing system, the propagation velocity of the shock wave at the first pulse was identical to the result for single-pulse operation. The propagation velocity was increased at the second pulse when the air supply was too small for full refilling. The velocity became steady at the third pulse and later pulses. Similarly, the impulse imparted by each pulse decreased at the second pulse and a steady impulse was obtained at later pulses. As a result, steady repetitive impulses were successfully generated in multipulse operation with a forced-breathing system.

Dependencies of the propagation velocity of the shock wave and thrust performance on a partial-filling rate were compared with the thrust-generation model with the partial filling of fresh air. The measured propagation velocity and thrust impulse showed good agreement with analytical predictions. The thrust impulse was identical to the thrust at the single-pulse operation when the partial-filling rate was unity, showing that the microwave rocket can be operated with no performance decrease with perfect air-filling.

Acknowledgment

This study was partially supported by a Ministry of Education, Culture, Sports, Science and Technology Grant-in-Aid for Japan Society for the Promotion of Science Fellows, 17-11856.

References

[1] Kantrowitz, A., "Propulsion to Orbit by Ground-based Lasers," *Astronautics and Aeronautics*, Vol. 10, No. 5, 1972, pp. 74–76.

[2] Myrabo, L. N., "World Record Flights of Beamed-Riding Rocket Lightcraft," AIAA Paper 2001-3798, 2001.

[3] Sashoh, A., Kister, M., Urabe, N., and Takayama, K., "Laser-Powered Launch in Tube," *Transactions of the Japan Society for Aeronautical and Space Sciences*, Vol. 46, No. 151, 2003, pp. 52–54. doi:10.2322/tjsass.46.52

[4] Phipps, C., and Luke, J., "Diode Laser-Driven Microthrusters: A New Departure for Micropropulsion," *AIAA Journal*, Vol. 40, No. 2, Feb. 2002, pp. 310–318. doi:10.2514/2.1647

[5] Katsurayama, H., Komurasaki, K., and Arakawa, Y., "Feasibility for the Orbital Launch by Pulse Laser Propulsion," *Journal of Space Technology and Science*, Vol. 20, No. 2, 2005, p. 32.

[6] Knecht, J. P., and Micci, M. M., "Analysis of a Microwave-Heated Planar Propagating Hydrogen Plasma," *AIAA Journal*, Vol. 26, No. 2, Feb. 1988, pp. 188–194. doi:10.2514/3.9871

[7] Batanov, G. M., Gritsinin, S. I., Kossyy, I. A., Magunov, A. N., Silakov, V. P., and Tarasova, N. M., *Plasma Physics and Plasma Electronics*, edited by L. M. Kovrizhnykh, Nova Science, Commack, NY, 1989, pp. 241–282.

[8] Parkin, K. L. G., and Culick, F. E. C., "Feasibility and Performance of the Microwave Thermal Rocket Launcher," *Proceedings of Second International Symposium on Beamed Energy Propulsion*, American Inst. of Physics, Melville, NY, 2003.

[9] Bruccoleri, A. R., Parkin, K. L. G., and Barmartz, M., "Axial Temperature Behavior of a Heat Exchanger Tube for Microwave Thermal Rockets," *Journal of Propulsion and Power*, Vol. 23, No. 4, 2007, pp. 889–894. doi:10.2514/1.27847

[10] Nakagawa, T., Mihara, Y., Komurasaki, K., Takahashi, K., Sakamoto, K., and Imai, T., "Propulsive Impulse Measurement of a Microwave-Boosted Vehicle in the Atmosphere," *Journal of Spacecraft and Rockets*, Vol. 41, No. 1, 2004, pp. 151–153. doi:10.2514/1.2540

[11] Oda, Y., Komurasaki, K., Takahashi, K., Kasugai, A., and Sakamoto, K., "Plasma Generation Using High-Power Millimeter Wave Beam and Its Application for Thrust Generation," *Journal of Applied Physics*, Vol. 100, No. 11, Dec. 2006, Paper 113308. doi:10.1063/1.2362908

[12] Oda, Y., Shibata, T., Komurasaki, K., Takahashi, K., Kasugai, A., and Sakamoto, K., "A Plasma and Shockwave Observation with Pulse Repetition in a Microwave Boosted Thruster," AIAA Paper 2006-4631, 2006.

[13] Bussing, T., and Pappas, G., "An Introduction to Pulse Detonation Engines," AIAA Paper 94-0263, 1994.

[14] Endo, T., Kasahara, J., Matsuo, A., Inaba, K., Sato, S., and Fujiwara, T., "Pressure History at the Thrust Wall of Simplified Pulse Detonation Engine," *AIAA Journal*, Vol. 42, No. 9, 2004, pp. 1921–1930. doi:10.2514/1.976

[15] Oda, Y., Shibata, T., Komurasaki, K., Takahashi, K., Kasugai, A., and Sakamoto, K., "A Thrust Generation Model of Microwave Rocket," *Journal of Space Technology and Science*, Vol. 22, No. 2, 2007, pp. 30–35.

[16] Kasugai, A., Sakamoto, K., Minami, R., Takahashi, K., and Imai, T., "Study of Millimeter Wave High-Power Gyrotron for Long Pulse Operation," *Nuclear Instruments and Methods in Physics Research*, Vol. 528, Nos. 1–2, Aug. 2004, pp. 110–114. doi:10.1016/j.nima.2004.04.029

[17] Sakamoto, K., Kasugai, A., Takahashi, K., Minami, R., Kobayashi, N., and Kajiwara, K., "Achievement of Robust High-Efficiency 1 MW Oscillation in the Hard-Self-Excitation Region by a 170 GHz Continuous-Wave Gyrotron," *Nature Physics*, Vol. 3, No. 6, 2007, pp. 411–414. doi:10.1038/nphys599

G. Spanjers
Associate Editor